

**SGLI/GCOM-C1**

**Algorithm Theoretical Basic Document**

**Phytoplankton functional type (PHFT)**

Version 3  
31 March 2016

PI: Toru Hirawake<sup>1\*</sup>  
Co-I: Amane Fujiwara<sup>2</sup>, Tomonori Isada<sup>3</sup> and Sei-ichi Saitoh<sup>1,4</sup>

<sup>1</sup> Faculty of Fisheries Sciences, Hokkaido University

<sup>2</sup> JAMSTEC

<sup>3</sup> Field Science Center, Hokkaido University

<sup>4</sup> Arctic Research Center, Hokkaido University

\*PI: [hirawake@salmon.fish.hokudai.ac.jp](mailto:hirawake@salmon.fish.hokudai.ac.jp)

Contributors

Hisatomo Waga, Faculty of Fisheries Sciences, Hokkaido University

Koji Suzuki, Faculty of Environmental Earth Sciences, Hokkaido University

This ATBD is based on Waga et al. " Distributional shifts in size structure of phytoplankton community" preparing to submit to Remote Sensing.

## 1. Algorithm outline

### 1.1 Algorithm Code

PHFT\_V3.f95

### 1.2 Product Code

PHFT (Phytoplankton functional type, research level product)

### 1.3 PI

Toru Hirawake (GCOM-C1 2nd RA 133, 4th RA 304)

### 1.4 Overview of algorithm

Phytoplankton functional types (PFTs) are phytoplankton groups classified based on their biogeochemical and ecological functions. Size distribution of phytoplankton is one of the PFTs and important factor to determine the structure of ecology, particularly a number of trophic levels in the ocean. This algorithm estimates abundance of each phytoplankton size classes (micro-, nano- and picoplankton) in their ratio and chlorophyll *a* (Chl *a*) concentration.

Phytoplankton size class has been modeled using one of inherent optical properties (IOPs) in the past studies; light absorption of phytoplankton [e.g. *Fishwick et al., 2006; Hirata et al., 2008*] and backscattering coefficient [e.g. *Montes-Hugo et al., 2008; Vaillancourt et al., 2004*]. While ratio of the absorption coefficient,  $a_{\text{ph}}(\lambda_1)/a_{\text{ph}}(\lambda_2)$ , tends to express pigment composition and packaging, spectral slope of the scattering coefficient,  $\gamma$ , is controlled by geometry of phytoplankton cell. To take the advantage of these IOPs, the size deriving model (SDM) using both the absorption ratio and  $\gamma$  was established in the Arctic Ocean and estimated the abundance of ultraplankton ( $< 5\mu\text{m}$ ) [*Fujiwara et al., 2011*].

In the previous RA (RA2), the SDM had been improved to estimate three size classes. However, dataset is quite limited because of difference in filter pore size among cruises and lack of backscattering data. Therefore, we applied the theory of particle size distribution [*Junge, 1963*] and estimated slope of chlorophyll size distribution (CSD) using only absorption coefficient of phytoplankton in the RA4.

The data set used in this study were obtained from a wide range of the North Pacific Ocean and the Western Arctic through fifteen cruises over a 9-year period (Figure 1). At each station, size fractionated Chla (Chlasize), light absorption coefficient and spectral radiation were measured. Seawater samples were collected

from the sea surface using a clean plastic bucket. Seventy percent of in situ data ( $N = 180$ ) were used for model development and the rest ( $N = 78$ ) was reserved for model validation.

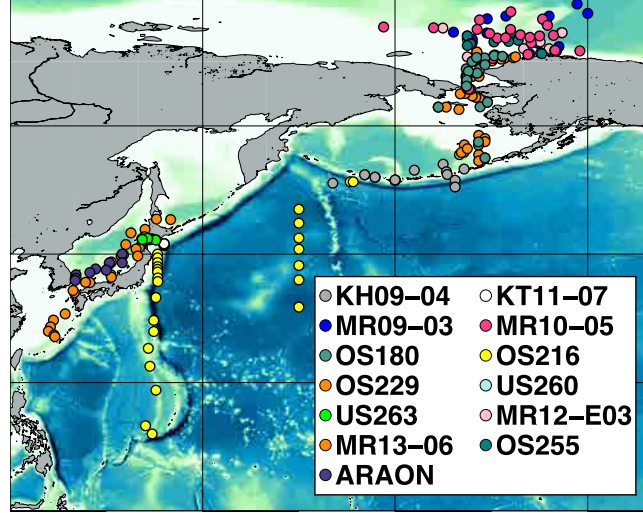


Figure 1. Map of sampling stations.

## 2. Theoretical Description

### 2.1. Basic of algorithm

Assuming that the PSD follows the Junge-type [Junge, 1963] power law size distribution [Bader, 1970], the number concentration of particles ( $N$ ) of particles per unit volume of seawater normalized by the size bin diameter ( $D$ ) can be expressed as follows:

$$N(D) = N_0 \left( \frac{D}{D_0} \right)^{-\xi}, \quad (1)$$

where  $\xi$  is the Junge slope of PSD, and  $D_0$  is a reference diameter at which  $N_0 = N(D_0)$ . Therefore, the total number of particles in a given size range can be derived as integrating Eq. (1) from the minimum diameter ( $D_{\min}$ ) to the maximum diameter ( $D_{\max}$ ) enabling the PSD to be partitioned into distinct classes, described by

$$N = \int_{D_{\text{mix}}}^{D_{\text{max}}} N_0 \left(\frac{D}{D_0}\right)^{-\xi} dD. \quad (2)$$

If assuming that the Chla is particle and thus the Chla size distribution (CSD) also follows the Junge-type power law distribution, the total Chla ( $\text{Chla}_{\text{total}}$ ) and  $\text{Chla}_{\text{size}}$  in a given size range from  $D_1$  to  $D_2$  can be expressed with Eq. (3) and (4) as follows:

$$\text{Chla}_{\text{total}} = \int_{D_{\text{min}}}^{D_{\text{max}}} \text{Chla}_0 \left(\frac{D}{D_0}\right)^{-\eta} dD, \quad (3)$$

$$\text{Chla}_{\text{size}} = \int_{D_1}^{D_2} \text{Chla}_0 \left(\frac{D}{D_0}\right)^{-\eta} dD, \quad (4)$$

where  $\text{Chla}_0$  is the reference Chla at  $D_0$  (here, 0.7  $\mu\text{m}$ ), and  $\eta$  is the exponent of Chla size spectrum (hereafter CSD slope). The strong magnitude of the CSD slope indicates the large proportion of smaller phytoplankton, while that of low magnitude suggests the larger phytoplankton dominant condition. In this study, we assumed  $D_{\text{min}}$  and  $D_{\text{max}}$  as the pore size of GF/F filter (i.e. 0.7  $\mu\text{m}$ ) and 200  $\mu\text{m}$  [Dussart, 1965], respectively. The CSD slope is derived as the slope of linear regression in log-space between the inverse log-transformed median diameters from log-transformed  $D_1$  to  $D_2$  and  $\text{Chla}_{\text{size}}$  normalized by the size bin width.

Note that the Chla fraction of arbitrarily defined size range ( $F_{\text{size}}$ ) can be derived using the CSD slope as follows:

$$F_{\text{size}} = 100 \times \frac{\text{Chla}_{\text{size}}}{\text{Chla}_{\text{total}}} = 100 \times \frac{\int_{D_1}^{D_2} \text{Chla}_0 \left(\frac{D}{D_0}\right)^{-\eta} dD}{\int_{0.7}^{200} \text{Chla}_0 \left(\frac{D}{D_0}\right)^{-\eta} dD} = 100 \times \frac{D_2^{1-\eta} - D_1^{1-\eta}}{200^{1-\eta} - 0.7^{1-\eta}}, \quad (5)$$

where the constants  $\text{Chla}_0$  and  $D_0$  no longer exist in Eq. (6), so that only the CSD slope and diameter range are required for estimating the each fraction of phytoplankton size classes.

## 2. 2. Quantification of CSD slope using phytoplankton absorption spectra

To quantify the CSD slope using the spectral shape of  $a_{\text{ph}}(\lambda)$ , we applied PCA to normalized  $a_{\text{ph}}(\lambda)$  following the method of Wang *et al.* [2015]. In brief, normalized  $a_{\text{ph}}(\lambda)$  ( $a_{\text{ph}}^{\text{std}}(\lambda)$ ) was derived from its wavelength mean and the standard deviation. The formula for  $a_{\text{ph}}^{\text{std}}(\lambda)$  is shown as below:

$$a_{\text{ph}}^{\text{std}}(\lambda) = \left[ a_{\text{ph}}(\lambda) - \text{mean}(a_{\text{ph}}(\lambda)) \right] / \text{std}(a_{\text{ph}}(\lambda)), \quad (6)$$

where  $\text{mean}(a_{\text{ph}}(\lambda))$  and  $\text{std}(a_{\text{ph}}(\lambda))$  are the wavelength mean and standard deviation of  $a_{\text{ph}}(\lambda)$ , respectively.

PCA was then applied to  $a_{\text{ph}}^{\text{std}}(\lambda)$  to capture spectral feature of phytoplankton absorption property. The input values for PCA was a matrix ( $m \times N$ ) constituted of  $a_{\text{ph}}^{\text{std}}(\lambda)$ , where  $m$  and  $N$  were the number of wavelengths and samples, respectively. The resulting PC scores were assumed to correlate with the CSD slope, and hence the CSD slope was quantified as the logistic-type regression model using  $i$ th PC score ( $S_i$ ) and regression coefficients between the CSD slope and PC scores ( $\beta_0$  and  $\beta_i$ ) as below:

$$\eta = \left[ \beta_0 + \exp \sum_{i=1}^k \beta_i S_i \right]^{-1}, \quad (7)$$

where  $k$  is the number of PCs. Here,  $S_i$  can also be express as follows:

$$S_i = \sum_{j=1}^m w_{i,j} a_{\text{ph}}^{\text{std}}(\lambda_j), \quad (8)$$

where  $w_{i,j}$  and  $a_{\text{ph}}^{\text{std}}(\lambda_j)$  are the loading factor for the  $i$ th PC and  $a_{\text{ph}}^{\text{std}}(\lambda)$  value at wavelength  $j$ , respectively. Therefore, we obtained an equation by substituting for calculation of  $S_i$  in Eq. (7):

$$\eta = \left[ \beta_0 + \exp \sum_{j=1}^m C_j a_{\text{ph}}^{\text{std}}(\lambda_j) \right]^{-1}, \quad (9)$$

$$C_j = \sum_{i=1}^k \beta_i w_{i,j}. \quad (10)$$

Finally, the CSD slope is derived from Eq. (9) using the model parameters of  $\beta_0$  and  $C_j$ .

The resulting model parameter  $\beta_0$  was -0.221 and  $C_j$  for each wavelengths at 412, 443, 469, 488, 531, 547 and 555 nm were -0.222 and 0.314, 0.021, -0.780, 0.243, 1.714, -0.189 and -1.305, respectively.

### 2. 3. Evaluation of estimate accuracy

The root-mean square error (*RMSE*) was adopted when we validated the agreement of two values such as measured and estimated CSD slope. The *RMSEs* were computed as relative values so as to give equal weights to all samples, and expressed as percentages [Ciotti *et al.*, 2006], described by

$$RMSE(\%) = 100 \times \sqrt{\frac{1}{N} \sum_{i=1}^N \left( \frac{Meas_i - Mod_i}{Meas_i} \right)^2}, \quad (11)$$

where  $Meas_i$  and  $Mod_i$  are  $i$ th measured and modelled values, respectively.

### 3 Validation

The performance of CSD model was examined by comparing measured CSD slope determined from in situ Chl<sub>a</sub> and modeled CSD slope estimated from in situ Rrs( $\lambda$ ). The resulting RMSE between measured and modeled CSD slope was 25.9% (Figure 2). Since CSD model relies on the spectrum shape of  $aph(\lambda)$ , the accuracy of estimated CSD slope strongly depends on the robustness of IOP algorithms. The satellite product accuracy goal for Chl<sub>a</sub> has been delimited the  $\pm 35\%$  of agreement with respect to actual value measured in the field [Hooker and McClain, 2000], and other products such as primary production were also evaluated based on this range. Moreover, the existing methods to derive phytoplankton size structure often use Chl<sub>a</sub> as an input data [Devred *et al.*, 2011; Hirata *et al.*, 2011; Brewin *et al.*, 2010] and are expected to contribute for understanding the biogeochemical process [McClain, 2009]. Therefore, the CSD model enabled to retrieve size structure of phytoplankton community with the same or better accuracy when comparing to Chl<sub>a</sub> and other products came from Chl<sub>a</sub>.

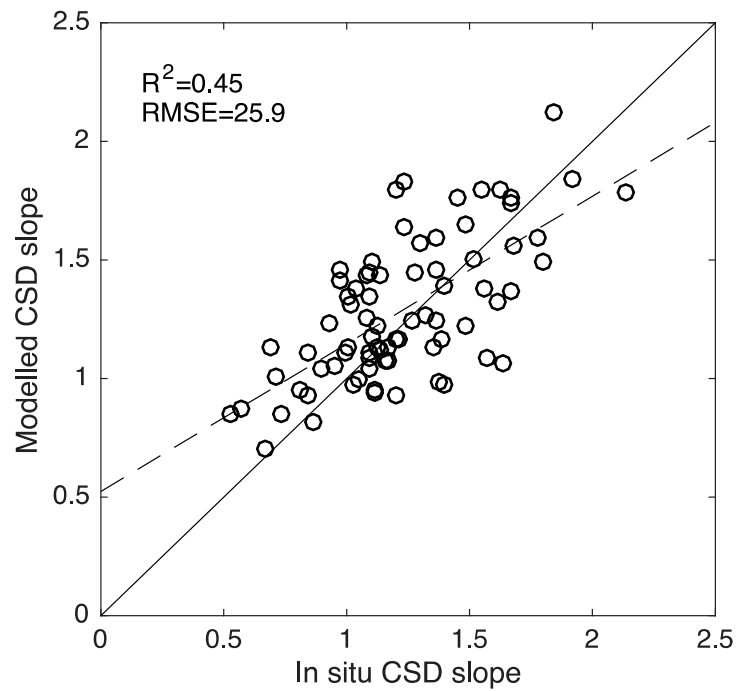


Figure 2. Comparison of in situ CSD slope determined from in situ  $Chl a_{size}$  and modelled CSD slope derived from estimated  $a_{ph}^{std}(\lambda)$  through QAA-v5 using in situ PRR data. Solid and dashed lined represent the 1:1 agreements and regression lines, respectively.

#### 4. References

- Bader, H. (1970), The hyperbolic distribution of particle sizes. *J. Geophys. Res.*, 75, 2822–2830.
- Brewin, R. J. W., Sathyendranath, S., Hirata, T., Lavender, S. J., Barciela, R. M., Hardman-Mountford, N. J. A (2010), Three-component model of phytoplankton size class for the Atlantic Ocean, *Ecol. Model.*, 221, 1472–1483.
- Ciotti, A. M., Bricaud, A. (2006), Retrievals of a size parameter for phytoplankton and spectral light absorption by colored detrital matter from water-leaving radiances at SeaWiFS channels in a continental shelf region off Brazil, *Limnol. Oceanogr. Methods*, 4, 237–253.
- Dussart, B. H. (1965), Les différentes catégories de plancton, *Hydrobiologia*, 26, 72–74.
- Devred, E., Sathyendranath, S., Stuart, V., Platt, T. (2011), A three component classification of phytoplankton absorption spectra: Application to ocean-color data, *Remote Sens. Environ.*, 115, 2255–2266.
- Fishwick, J. R., J. Aiken, R. Barlow, H. Sessions, S. Bernard, and J. Ras (2006), Functional relationships and bio-optical properties derived from phytoplankton pigments, optical and photosynthetic parameters; a case study of the Benguela ecosystem, *Journal of the Marine Biological Association of the United Kingdom*, 86(06), 1267-1280.
- Fujiwara, A., T. Hirawake, K. Suzuki, and S. I. Saitoh (2011), Remote sensing of size structure of phytoplankton communities using optical properties of the Chukchi and Bering Sea shelf region, *Biogeosciences Discuss.*, 8(3), 4985-5017.
- Hirata, T., J. Aiken, N. Hardman-Mountford, T. J. Smyth, and R. G. Barlow (2008), An absorption model to determine phytoplankton size classes from satellite ocean colour, *Remote Sensing of Environment*, 112, 3153-3159.
- Hirata, T., Hardman-Mountford, N. J., Brewin, R. J. W., Aiken, J., Barlow, R., Suzuki, K., Isada, T., Howell, E., Hashioka, T., Noguchi-Aita, M., et al. (2011), Synoptic relationships between surface Chlorophyll-*a* and diagnostic pigments specific to phytoplankton functional types, *Biogeosciences*, 8, 311–327.
- Hooker, S. B., McClain, C. R. (2000), The calibration and validation of SeaWiFS data. *Prog. Oceanogr.*, 45, 427–465.

- Junge, C. E. (1963), Air chemistry and radioactivity. New York and London: Academic Press Inc., 382
- McClain, C. R. (2009), A decade of satellite ocean color observations. *Annu. Rev. Marine. Sci.*.
- Montes-Hugo, M. A., M. Vernet, R. Smith, and K. Carder (2008), Phytoplankton size-structure on the western shelf of the Antarctic Peninsula: a remote-sensing approach, *International Journal of Remote Sensing*, 29(3), 801-829.
- Vaillancourt, R. D., C. W. Brown, R. R. L. Guillard, and W. M. Balch (2004), Light backscattering properties of marine phytoplankton: relationships to cell size, chemical composition and taxonomy, *J Plankton Res*, 26, 191-212.
- Wang, S., Ishizaka, J., Hirawake, T., Watanabe, Y., Zhu, Y., Hayashi, M., Yoo, S. (2015), Remote estimation of phytoplankton size fractions using the spectral shape of light absorption, *Opt. Express*, 23, 10301–10318.